

## Effect of Photosensitizer Dose on Fluence Rate Responses to Photodynamic Therapy<sup>†</sup>

Hsing-Wen Wang<sup>1,2</sup>, Elizabeth Rickter<sup>1</sup>, Min Yuan<sup>1</sup>, E. Paul Wileyto<sup>3</sup>, Eli Glatstein<sup>1</sup>, Arjun Yodh<sup>2</sup> and Theresa M. Busch<sup>\*1</sup>

<sup>1</sup>Department of Radiation Oncology, School of Medicine, University of Pennsylvania, Philadelphia, PA

<sup>2</sup>Department of Physics and Astronomy, School of Arts and Sciences, University of Pennsylvania, Philadelphia, PA

<sup>3</sup>Tobacco Use Research Center, School of Medicine, University of Pennsylvania, Philadelphia, PA

Received 23 December 2006; accepted 19 March 2007; DOI: 10.1111/j.1751-1097.2007.00139.x

### ABSTRACT

Photodynamic therapy (PDT) regimens that conserve tumor oxygenation are typically more efficacious, but require longer treatment times. This makes them clinically unfavorable. In this report, the inverse pairing of fluence rate and photosensitizer dose is investigated as a means of controlling oxygen depletion and benefiting therapeutic response to PDT under conditions of constant treatment time. Studies were performed for Photofrin-PDT of radiation-induced fibrosarcoma tumors over fluence rate and drug dose ranges of 25–225 mW cm<sup>-2</sup> and 2.5–10 mg kg<sup>-1</sup>, respectively, for 30 min of treatment. Tumor response was similar among all inverse regimens tested, and, in general, tumor hemoglobin oxygen saturation (SO<sub>2</sub>) was well conserved during PDT, although the highest fluence rate regimen (225 mW × 2.5 mg) did lead to a modest but significant reduction in SO<sub>2</sub>. Regardless, significant direct tumor cell kill (> 1 log) was detected during 225 mW × 2.5 mg PDT, and minimal normal tissue toxicity was found. PDT effect on tumor oxygenation was highly associated with tumor response at 225 mW × 2.5 mg, as well as in all other regimens tested. These data suggest that high fluence rate PDT can be carried out under oxygen-conserving, efficacious conditions at low photosensitizer dose. Clinical confirmation and application of these results will be possible through use of minimally invasive oxygen and photosensitizer monitoring technologies, which are currently under development.

### INTRODUCTION

The therapeutic benefits of conserving tumor oxygenation during photodynamic therapy (PDT) are well known. Treatment regimens that lead to less oxygen depletion during illumination are more efficient (1). Preclinical studies demonstrate oxygen-conserving protocols to result in more tumor damage, longer tumor growth delays and/or a higher percentage of tumor cures (2–5). Normal tissue toxicity is also reduced during oxygen-conserving PDT under the condition that total dose is reduced to compensate for the enhanced efficiency of

the oxygen-conserving regimen (6). Clinical investigation confirms that treatment at lower fluence rate, which is associated with better oxygen maintenance during PDT, leads to a greater number of complete responses (7).

Among the factors affecting oxygen depletion during PDT are light delivery method (continuous vs fractionated), intensity of light delivery (fluence rate), tissue photosensitizer level, photosensitizer type and tumor microenvironment (intracapillary spacing, hemoglobin oxygen saturation, etc.) (8–11). Hyperfractionated illumination, *i.e.* rapid cycles of alternating illumination and dark periods, facilitates the recovery of tissue oxygenation during the dark periods. Lower fluence rates favor oxygen maintenance during PDT by reducing the singlet oxygen production rate and thus the rate of ground state oxygen consumption. Replenishment of tissue oxygen through the blood flow can more effectively keep pace with oxygen consumption during low compared with high fluence rate PDT. As with fluence rate, lower tissue photosensitizer concentration enables better oxygen maintenance by reducing the amount of singlet oxygen produced per unit of time. Photosensitizer type affects oxygen consumption through drug photophysical characteristics; drugs with higher extinction coefficients at the treatment wavelength or higher quantum yields for singlet oxygen production will cause more rapid oxygen depletion. Finally, tumor microenvironment contributes to oxygenation during PDT through its effects on oxygen delivery.

In translational research, most investigations have focused on manipulation of light delivery, either through use of lower fluence rate or fractionated illumination, to control oxygen depletion during PDT (2,4,12,13). A negative aspect of these methods is the need to increase treatment times for delivery of an equally effective PDT dose under oxygen-conserving conditions (6). In clinical applications, especially those in which PDT is performed intraoperatively, long treatment times are unacceptable. For this reason, it is not uncommon for higher fluence rates to be employed in clinical trials; lowering fluence rate or fractionating the dose is not considered an option, even for the purpose of oxygen conservation (1). Importantly though, clinical trials also routinely use lower photosensitizer doses than preclinical studies, and in theory lower tumor drug levels could counterbalance the oxygen-consuming properties of high fluence rate (14,15).

<sup>†</sup>This invited paper is part of the Symposium-in-Print: Photodynamic Therapy.

\*Corresponding author email: buschtm@mail.med.upenn.edu

(Theresa M. Busch)

© 2007 The Authors. Journal Compilation. The Society of Photobiology 0031-8655/07

Despite its pertinence to clinical PDT, few studies have investigated the PDT effect of fluence rate manipulation in combination with photosensitizer dose adjustment. In this report, we investigate how rationally designed inverse pairing of fluence rate and photosensitizer dose affects tumor oxygenation and therapeutic response to PDT under conditions of constant treatment time. These investigations have two primary purposes: (1) to evaluate whether pairing of increasing fluence rate with decreasing photosensitizer dose will provide efficacious response in the presence of oxygen conservation during PDT and (2) to determine if PDT effect on tumor oxygenation is directly correlated with response across the inversely paired treatment regimens.

## MATERIALS AND METHODS

**Tumor model and PDT.** Radiation-induced fibrosarcoma (RIF) tumors were propagated on the shoulders of 9- to 11-week-old C3H mice (NCI-Frederick, Frederick, MD or Taconic; Germantown, NY) by the intradermal injection of  $3 \times 10^5$  cells. Animals received PDT or control treatment  $\sim 7$ –9 days later when tumors reached a volume appropriate for each experimental endpoint; tumors of volume  $\leq 100 \text{ mm}^3$  were used in tumor-response studies, whereas tumors  $\sim 100$ – $175 \text{ mm}^3$  in volume were used for investigations requiring tumor excision, e.g. *in vivo/in vitro* clonogenic assay, in order to ensure sufficient sample for analysis. The photosensitizer Photofrin (Axcan Pharma Inc., Mont-Saint-Hilaire, QC, Canada) was administered *via* tail vein at  $\sim 24$  h prior to illumination at doses specified in the Results. Tumor concentration of photosensitizer was measured by spectrofluorometric assay, following a procedure previously published (16). Illumination of a shaved and depilated (Nair<sup>®</sup>) treatment field was performed using a KTP Yag pumped dye module (Laserscope, San Jose, CA) tuned to produce 630 nm of light. Light was delivered through microlens-tipped fibers (CardioFocus, Norton, MA) to produce an illumination area of 1.0–1.1 cm diameter, depending on tumor size. Laser output was measured with a power meter (Coherent, Auburn, CA) and adjusted as needed to produce fluence rates in the range of 25–225  $\text{mW cm}^{-2}$  as specified in the Results. Treatment fluence was varied as required to maintain a constant treatment time of 30 min at all fluence rates. Controls included animals receiving only light (no photosensitizer), only Photofrin (no light) and untreated (neither photosensitizer nor light). During PDT- or control-treatment, mice were anesthetized by inhalation of isoflurane in medical air, delivered through a nose cone (VetEquip anesthesia machine, Pleasanton, CA).

**Tumor-response assay.** PDT was performed over a 1 cm diameter area centered on RIF tumors of  $\leq 100 \text{ mm}^3$  in volume. After PDT- or control-treatment, mice were followed daily to determine the number of days after treatment until tumor volume equaled or exceeded  $400 \text{ mm}^3$  (time-to- $400 \text{ mm}^3$ ). Tumor volume was measured in two orthogonal directions and calculated using the formula volume = diameter  $\times$  width<sup>2</sup>  $\times 3.14/6$ . A cure was defined as no sign of tumor regrowth at 90 days after PDT; cures were treated as censored data points for the purpose of statistical analysis.

**In vivo optical (diffuse reflectance) spectroscopy.** A continuous wave broadband reflectance spectroscopy system was used to measure tumor optical properties and from these optical properties, tumor total hemoglobin concentration (THC) and hemoglobin oxygen saturation ( $\text{SO}_2$ ) were calculated. Optical measurements were performed immediately before and immediately after PDT in each animal with  $\sim 10$ – $20$  spatially distributed measurements (acquisition time of 100 ms/measurement) collected at each timepoint. The sampling incorporated tissue up to  $\sim 2$  mm in depth, thus optical measurements were well averaged within a tumor. The instrumentation, theory and application of the spectroscopy system has been described in detail in previous reports (17–20). Briefly, the system consists of a 250 W quartz tungsten halogen lamp (Cuda Fiberoptics, Jacksonville, FL), a handheld surface contact fiber-optic probe, a monochromator (Acton Research, Acton, MA) to disperse light from the detection fibers and a liquid nitrogen-cooled CCD camera (Roper Scientific, Trenton, NJ) to image the reflectance spectra from multiple detection fibers simultaneously. Spectra were collected in the 600–800 nm wavelength range and

calibrated based on measurements in a 6 inch diameter integrating sphere (LabSphere Inc., North Sutton, NH) (18,19,21). Data were fit by an algorithm based on the diffusion equation with the restriction that  $\mu_s' = A\lambda^{-B}$  and  $\mu_a = \sum c_i \epsilon_i(\lambda)$ , where  $\lambda$  is the wavelength and  $c_i$  and  $\epsilon_i$  are the concentration and extinction coefficient of the  $i$ th chromophore, respectively. Primary chromophores considered were oxyhemoglobin ( $\text{HbO}_2$ ), deoxyhemoglobin (Hb), Photofrin and water; the extinction coefficients of  $\text{HbO}_2$ , Hb and water were obtained from the literature (22) and the extinction coefficient of Photofrin was obtained by direct measurement using an absorption spectrometer (Ocean Optics, Dunedin, FL). The diffuse reflectance algorithm simultaneously fit data from all wavelengths and source-detector separations to analytical solutions of the photon diffusion equation for a semi-infinite turbid medium (23–30), in order to extract  $A$ ,  $B$ ,  $c_{\text{Photofrin}}$ ,  $c_{\text{water}}$ ,  $c_{\text{HbO}_2}$  and  $c_{\text{Hb}}$ . From these quantities, we calculated tumor THC ( $\text{THC} = c_{\text{HbO}_2} + c_{\text{Hb}}$ ) and tissue hemoglobin oxygen saturation ( $\text{SO}_2 = c_{\text{HbO}_2}/\text{THC}$ ). *Relative-SO<sub>2</sub>* was calculated as the ratio of  $\text{SO}_2$  after to before PDT in the same tumor. Although  $c_{\text{Photofrin}}$  and  $c_{\text{water}}$  were extracted outputs in the fitting process, the absorption coefficients of Photofrin and water are relatively small compared with those of  $\text{HbO}_2$  and Hb in tissue; we have found previously that the extracted  $c_{\text{HbO}_2}$  and  $c_{\text{Hb}}$  are quite insensitive to the extracted quantities for Photofrin and water (17).

**In vivo/in vitro clonogenic assay.** PDT was performed over a 1.1 cm diameter area centered on RIF tumors of  $\sim 100$ – $175 \text{ mm}^3$  in volume. At times immediately, 5 and 17 h after PDT animals were killed by  $\text{CO}_2$  inhalation and tumors were excised and enzymatically digested to a single cell suspension. This involved placing the weighed and minced tumor sample in a trypsinizing flask containing 3000 U deoxyribonuclease (Sigma-Aldrich, St. Louis, MO), 2000 U collagenase (Sigma-Aldrich) and 3 mg protease (Sigma-Aldrich) dissolved in 12 mL of Hank's Balanced Salt Solution. Samples were spun at low speed for 30 min at  $37^\circ\text{C}$ , with an interruption after 15 min in order to mix the suspension by pipette. The digested sample was passed through a cell strainer, centrifuged, resuspended in complete media (defined below) and counted. Cells were plated on 100 mm tissue culture dishes in triplicate at specific concentrations. The plating media, *i.e.* complete media, consisted of Minimum Essential Media Alpha (Gibco, Grand Island, NY) supplemented with 10% fetal calf serum (Atlanta Biologicals, Lawrenceville, GA), 100 U/mL penicillin G sodium (Gibco), 100  $\mu\text{g mL}^{-1}$  streptomycin sulfate (Gibco) and 300  $\mu\text{M}$  of L-glutamine (Gibco). After  $\sim 10$  days of incubation ( $37^\circ\text{C}$  at 5%  $\text{CO}_2$ ) for colony growth, cells were fixed and stained using methylene blue (2.5  $\text{mg mL}^{-1}$ ) dissolved in 30% alcohol. Colonies were counted and averaged over triplicate plates. The number of clonogenic cells/g was calculated as the number of cells per g of tumor times the ratio of the number of colonies counted to the number plated.

**Normal tissue toxicity.** Anesthetized mice received PDT over a 1 cm area on their depilated hindfoot. After PDT- or control-treatment, mouse foot response was scored using the scale listed in Table 1. Foot response was followed daily for 7 days and then five times a week thereafter until all feet returned to normal. A score of 2, which would require animal euthanasia, was not found for any of the mice treated in these investigations.

**Table 1.** Foot-response scoring system.

Numerical score*	Appearance
0	No apparent difference from normal
0.1	Very slight edema and/or erythema
0.3	Slight edema and/or erythema
0.5	Moderate edema and/or erythema
0.75	Large edema and/or erythema
1	Large edema and/or erythema with exudate
1.2	Erythema with slight scaly or crusty appearance
1.5	Erythema with definite scaly or crusty appearance
1.65	Slight damage to toes
1.75	Definite damage and/or slight fusion of toes
2.0†	Most toes fused but general shape unchanged

\*Scale is continuous thus intermediate scores are also possible.

†At scores of two mice are killed.

**Statistics.** Survival data were fitted with a Cox-regression model. Where needed, pair-wise comparisons of tumor responses between selected treatment regimens (hazard ratios) were made using the Wald test. The association between tumor response and PDT-induced change in tumor oxygenation was evaluated by plotting time-to-400 mm<sup>3</sup> vs *relative-SO<sub>2</sub>* and fitting the data with a linear model; the strength of the association was assessed by the correlation coefficient (*r*<sup>2</sup>) with statistical significance given by a Wald test comparing the estimated slope to a slope of 0. A sign-rank test was used to test for differences between the normalized fraction of SO<sub>2</sub> (*relative-SO<sub>2</sub>*) or the normalized difference in THC and the null hypothesis, *i.e.* a value of 1 or 0, respectively. A Wilcoxon rank-sum test was used for all other comparisons. A *P*-value of <0.05 was considered significant for all but the Cox-regression analysis. In this case, a Bonferroni correction was incorporated for the multiple comparisons, which resulted in significance at *P* < 0.008.

## RESULTS

### Tumor response to inverse fluence rate × photosensitizer dosing

We began these investigations by determining the therapeutic consequences of pairing increasing fluence rate with decreasing photosensitizer dose. A low PDT fluence rate of 25 mW cm<sup>-2</sup> and a high PDT fluence rate of 225 mW cm<sup>-2</sup> were chosen as three-fold lower and higher than our typical preclinical fluence rate of 75 mW cm<sup>-2</sup>. This nine-fold range in fluence rate adequately covers those most commonly employed in preclinical and clinical PDT. Photosensitizing conditions to pair with these fluence rates were chosen as those that produced an ~nine-fold difference in RIF drug concentration. The measured RIF Photofrin concentrations resulting from 10, 3 and 2.5 mg kg<sup>-1</sup> animal injections were 13 ± 3.7, 2.0 ± 0.3 and 1.3 ± 0.08 ng mg<sup>-1</sup>, respectively. Based on these data, a low drug dose of 2.5 mg kg<sup>-1</sup> and a high drug dose of 10 mg kg<sup>-1</sup> were chosen for investigation. A drug dose of 2.5 mg kg<sup>-1</sup> was paired with 225 mW cm<sup>-2</sup> and a drug dose of 10 mg kg<sup>-1</sup> was paired with 25 mW cm<sup>-2</sup>.

A tumor-response assay was used to compare the therapeutic efficacy of the designed fluence rate and photosensitizer dose pairs for treatments of equivalent length (30 min). Kaplan–Meier curves (Fig. 1a) demonstrate that PDT at a fluence rate of 225 mW cm<sup>-2</sup> with a drug dose of 2.5 mg kg<sup>-1</sup>

(225 mW × 2.5 mg) produced a similar effect to PDT at a fluence rate of 25 mW cm<sup>-2</sup> with a drug dose of 10 mg kg<sup>-1</sup> (25 mW × 10 mg). After 25 mW × 10 mg PDT, median time of tumor regrowth to 400 mm<sup>3</sup> (time-to-400 mm<sup>3</sup>) was 12.5 days and 1 cure occurred among 10 animals treated. After 225 mW × 2.5 mg PDT, median time-to-400 mm<sup>3</sup> was 12.5 days and no cures (*n* = 10) were found. Lowering the photosensitizer dose at either of the fluence rates led to substantial reductions in treatment efficacy. At 225 mW cm<sup>-2</sup> reducing the drug dose to 1 mg kg<sup>-1</sup> resulted in a median time-to-400 mm<sup>3</sup> of 7 days (1 cure of *n* = 7). At 25 mW cm<sup>-2</sup> lowering the drug dose to 5 mg kg<sup>-1</sup> resulted in a median time-to-400 mm<sup>3</sup> of 5 days (0 cures of *n* = 9). Tumor responses to PDT at 225 mW × 1 mg and 25 mW × 5 mg were no different from the growth of size-matched untreated RIF tumors (median time-to-400 mm<sup>3</sup> of 7 days). Light controls at 225 mW cm<sup>-2</sup> and drug controls with 10 mg kg<sup>-1</sup> Photofrin also produced short regrowth times (median time-to-400 mm<sup>3</sup> of 4 and 3 days, respectively). On the other hand, tumor responses at 225 mW × 2.5 mg and 25 mW × 10 mg were both significantly different from the untreated controls (*P* < 0.001 for both).

Studies were expanded to include intermediate fluence rates and photosensitizer doses because similar tumor response was found for PDT at 25 mW × 10 mg and 225 mW × 2.5 mg. Based on the fact that 25 mW × 10 mg and 225 mW × 2.5 mg were both efficacious, a three-fold increase in fluence rate was paired with a two-fold decrease in photosensitizer dose. In this manner, intermediate conditions of 75 mW × 5 mg and 150 mW × 3.5 mg were designed. Kaplan–Meier curves (Fig. 1b) demonstrate that tumor responses at 75 mW × 5 mg and 150 mW × 3.5 mg were very similar to those found at the lowest fluence rate (25 mW × 10 mg) and highest fluence rate (225 mW × 2.5 mg) regimen. Among these four conditions median time-to-400 mm<sup>3</sup> ranged from 12.5 to 19 days with 0–1 animal cured per treatment group (0–11% cure rates); no significant difference was detected between the condition with the longest median time-to-400 mm<sup>3</sup> (75 mW × 5 mg) and either of the conditions with the shortest median time-to-400 mm<sup>3</sup> (225 mW × 2.5 mg and 25 mW × 10 mg).

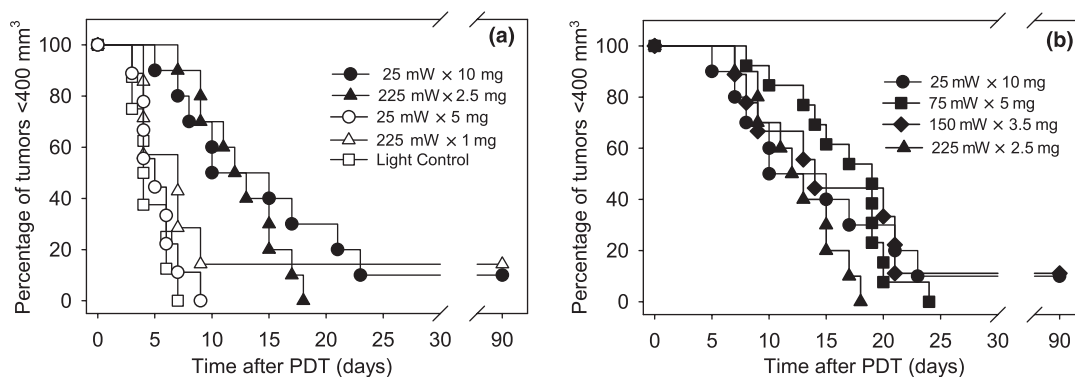


**Figure 1.** Kaplan–Meier curves of tumor responses to PDT with high vs low fluence rate (a) and at inverse fluence rate × photosensitizer dosing (b). Treatment conditions are abbreviated as fluence rate (mW) × photosensitizer dose (mg) for fluence rate units of mW cm<sup>-2</sup> and photosensitizer dose units of mg kg<sup>-1</sup>. Illumination (630 nm) was for 30 min at ~24 h after *i.v.* Photofrin injection; light controls received 225 mW cm<sup>-2</sup> illumination, but no Photofrin injection. Solid symbols indicate regimens of inverse fluence rate × photosensitizer dosing, calculated based on fluence rate and photosensitizer dose range that produced an ~nine-fold difference in delivered light intensity and tumor drug uptake, respectively. Open symbols indicate treatment regimens utilizing lower photosensitizer doses. *n* = 7–13 animals/condition.

### PDT effect on tumor hemoglobin oxygen saturation

The rationale behind pairing increasing fluence rate with decreasing photosensitizer dose was to facilitate maintenance of tumor oxygenation during high fluence rate PDT. The above tumor-response studies found high fluence rate  $\times$  low photosensitizer dose pairs to be equally efficacious as low fluence rate  $\times$  high photosensitizer dose in treatments of equivalent length. Next, we evaluated whether these isoeffective treatment regimens enabled conservation of tumor oxygenation during PDT.

*In vivo* optical spectroscopy was used to measure tumor hemoglobin oxygen saturation ( $SO_2$ ) immediately before and after PDT, and the effect of treatment on tumor oxygenation was reported as *relative-SO<sub>2</sub>*, which is the normalized change in  $SO_2$  ( $SO_2$  after PDT/ $SO_2$  before PDT) (Fig. 2). Thus, a *relative-SO<sub>2</sub>* value of 1 indicates no change in oxygenation relative to baseline (pre-PDT) levels. The highest fluence rate regimen (225 mW  $\times$  2.5 mg) did lead to some oxygen depletion during illumination: median *relative-SO<sub>2</sub>* (SE) was  $0.86 \pm 0.12$ , which was statistically different ( $P = 0.037$ ) from a value of 1. At the lower fluence rate regimens of 150 mW  $\times$  3.5 mg, 75 mW  $\times$  5 mg and 25 mW  $\times$  10 mg, median *relative-SO<sub>2</sub>* values were  $1.12 \pm 0.17$ ,  $1.26 \pm 0.11$  and  $1.04 \pm 0.21$ , respectively. These values suggest that hemoglobin oxygen saturation actually improved slightly at treatment conclusion, but only the 75 mW  $\times$  5 mg regimen was significantly ( $P = 0.040$ ) greater than a value of 1. Animals that were cured by PDT both exhibited *relative-SO<sub>2</sub>* values of  $\geq 2$  (see markers on the 150 mW  $\times$  3.5 mg and 25 mW  $\times$  10 mg plots). Two additional animals with *relative-SO<sub>2</sub>* values of  $\geq 2$  demonstrated long times to tumor regrowth, 24 and 21 days after PDT at 75 mW  $\times$  5 mg and 25 mW  $\times$  10 mg, respectively.

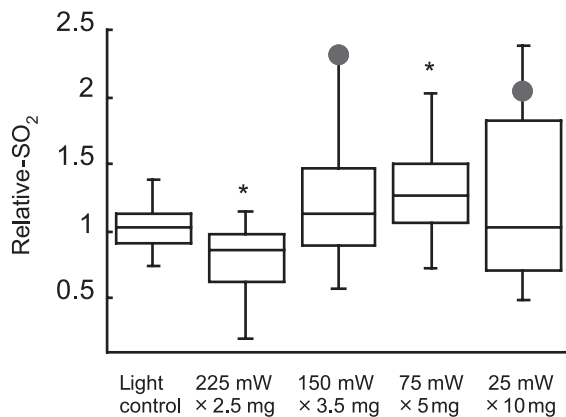


**Figure 2.** PDT effect on tumor hemoglobin oxygen saturation during treatment with inverse fluence rate  $\times$  photosensitizer dosing (box plots). *Relative-SO<sub>2</sub>* was measured as tumor  $SO_2$  after PDT normalized to the pre-PDT value in the same animal. Treatment conditions are abbreviated as fluence rate (mW)  $\times$  photosensitizer dose (mg) for fluence rate units of  $mW\ cm^{-2}$  and photosensitizer dose units of  $mg\ kg^{-1}$ . Illumination (630 nm) was for 30 min at  $\sim 24$  h after i.v. Photofrin injection; light controls received  $225\ mW\ cm^{-2}$  illumination, but no Photofrin injection. Markers indicate the *relative-SO<sub>2</sub>* values of animals that were cured.  $n = 8$ –13 animals/condition; \* indicates  $P < 0.05$  (sign-rank test) for a difference from a ratio of 1.

### Correlation between tumor response and PDT effect on hemoglobin oxygen saturation

We hypothesized that the therapeutic efficacy of inverse fluence rate  $\times$  photosensitizer dosing was related to its effectiveness at maintaining tumor oxygenation during illumination. In order to test this hypothesis, we evaluated the association between response durability (time-to-400  $mm^3$ ) and *relative-SO<sub>2</sub>*. Figure 3, panels a–d, plot time-to-400  $mm^3$  vs *relative-SO<sub>2</sub>* for animals treated with 225 mW  $\times$  2.5 mg, 150 mW  $\times$  3.5 mg, 75 mW  $\times$  5 mg and 25 mW  $\times$  10 mg, respectively. Within all treatment regimens, a significant association ( $P < 0.048$ ) was detected between response durability and the PDT-induced change in tumor hemoglobin oxygen saturation whereby increasing *relative-SO<sub>2</sub>* predicted for a better tumor response. Furthermore, all four of these treatment regimens could be fit by a single model (Fig. 3e;  $P = 7.971 \times 10^{-10}$ ).

Control animals receiving only illumination at 225 mW (no photosensitizer) demonstrated no association between *relative-SO<sub>2</sub>* and time-to-400  $mm^3$ , which establishes that relative oxygen levels do not independently predict for tumor growth (data not shown). Therefore, as to be expected, we also found no association between *relative-SO<sub>2</sub>* and time-to-400  $mm^3$  for treatment regimens that failed to have any PDT effect (225 mW  $\times$  1 mg and 25 mW  $\times$  5 mg; data not shown).

### Mechanisms of tumor damage

PDT-created tumor cell death at 25 mW  $\times$  10 mg vs 225 mW  $\times$  2.5 mg was studied using an *in vivo/in vitro* clonogenic assay. The data (Fig. 4) show PDT at 225 mW  $\times$  2.5 mg produced over one log ( $P < 0.021$ ) of cell kill in tumors excised immediately after PDT, which suggests the presence of substantial direct singlet oxygen-mediated cell damage during illumination. In contrast, 25 mW  $\times$  10 mg led to only insignificant cell death immediately after PDT. However, cell kill gradually increased as a function of time after treatment conclusion, and a significant decrease in tumor clonogenicity was detectable by 17 h after 25 mW  $\times$  10 mg PDT. No differences in tumor clonogenicity were found among control conditions of untreated tumor, illumination only (no photosensitizer) at  $225\ mW\ cm^{-2}$ , illumination only at  $25\ mW\ cm^{-2}$  and photosensitizer only (no illumination) at  $10\ mg\ kg^{-1}$  Photofrin.

In order to investigate how PDT effect on tumor blood flow may have contributed to differences in direct cell kill at 25 mW  $\times$  10 mg vs 225 mW  $\times$  2.5 mg, *in vivo* optical spectroscopy was used to measure THC in tumors prior to and immediately after PDT. During PDT at 25 mW  $\times$  10 mg, the median ( $\pm$ SE) change in THC among the individual tumors was a decrease of  $28 \pm 12\ \mu M$ , from an average ( $\pm$ SE) pre-PDT value of  $139 \pm 18\ \mu M$  to a post-PDT value of  $114 \pm 13\ \mu M$ . This bordered on a significant change ( $P = 0.064$ ) in hemoglobin concentration, suggesting the presence of PDT-created reductions in vascular perfusion during the 25 mW  $\times$  10 mg regimen. In contrast, minimal change in THC was found during PDT at 225 mW  $\times$  2.5 mg; a median ( $\pm$ SE) increase of  $5 \pm 8\ \mu M$  was measured (pre-PDT value  $122 \pm 5\ \mu M$ ; post-PDT value  $125 \pm 9\ \mu M$ ).

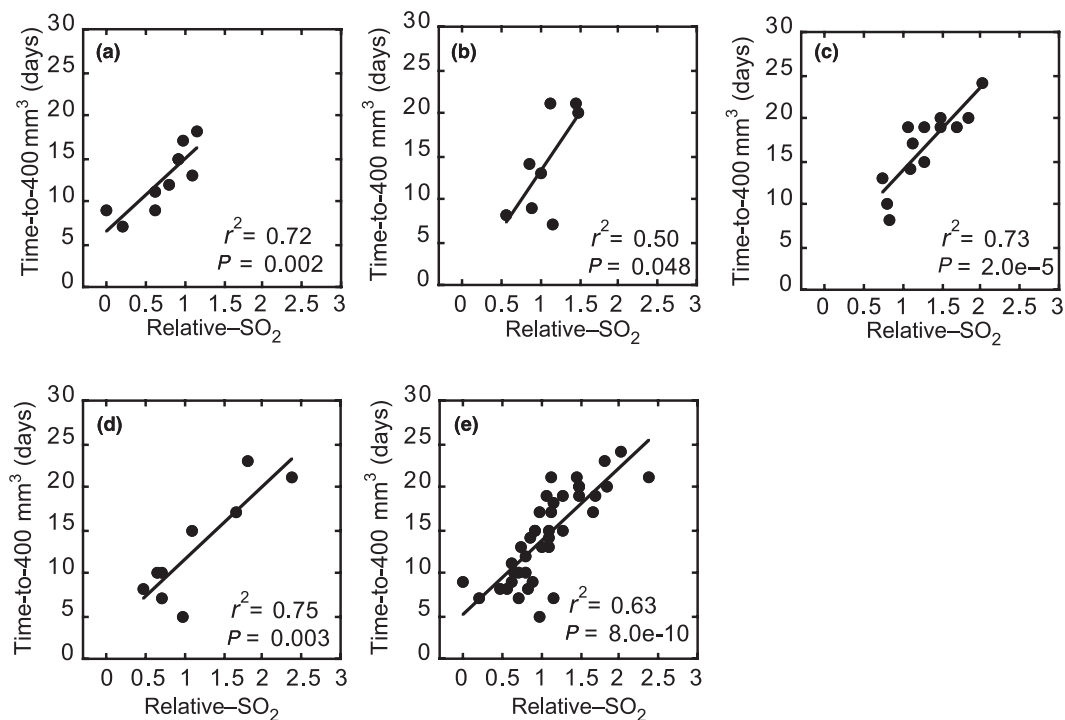


**Figure 3.** The association between tumor response and PDT effect on tumor hemoglobin oxygen saturation for treatment regimens of 225 mW cm<sup>-2</sup>, 2.5 mg kg<sup>-1</sup> Photofrin (a); 150 mW cm<sup>-2</sup>, 3.5 mg kg<sup>-1</sup> Photofrin (b); 75 mW cm<sup>-2</sup>, 5.0 mg kg<sup>-1</sup> Photofrin (c); 25 mW cm<sup>-2</sup>, 10 mg kg<sup>-1</sup> Photofrin (d); and all of the above (e). Tumor response was measured as the number of days after PDT until tumor regrowth to 400 mm<sup>3</sup> (time-to-400 mm<sup>3</sup>). PDT effect on hemoglobin oxygen saturation was measured as tumor SO<sub>2</sub> after PDT normalized to the pre-PDT value in the same animal (*relative-SO<sub>2</sub>*). Each data point indicates an individual animal. PDT illumination (630 nm) was for 30 min at ~24 h after i.v. Photofrin injection. The correlation coefficient (*r*<sup>2</sup>) and *P*-value (by a Wald test) of a linear fit to the data is indicated for each plot.

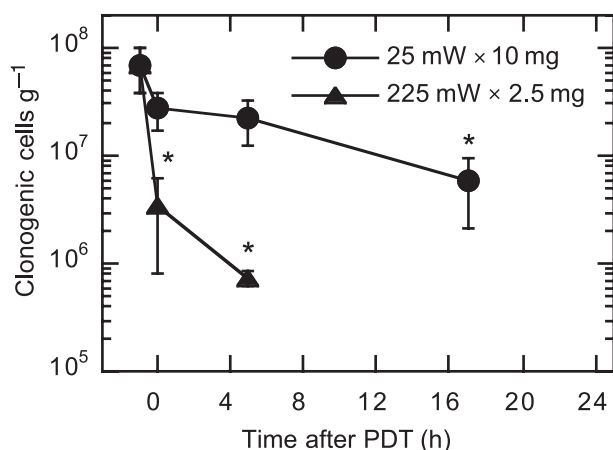


**Figure 4.** *In vivo/in vitro* clonogenic assay of tumor cell death after PDT at 25 mW cm<sup>-2</sup>, 10 mg kg<sup>-1</sup> Photofrin (25 mW × 10 mg) and 225 mW cm<sup>-2</sup>, 2.5 mg kg<sup>-1</sup> Photofrin (225 mW × 2.5 mg). Illumination (630 nm) was for 30 min at ~24 h after i.v. Photofrin injection. Points indicate mean (±SE) clonogenic cells/g of tumor. Data point at -1 h represents an average of control conditions (untreated tumor, 10 mg kg<sup>-1</sup> drug only, 25 mW cm<sup>-2</sup> light only and 225 mW cm<sup>-2</sup> light only). *n* = 3-5 animals/condition; \* indicates *P* < 0.05 (rank-sum test) for a difference from control conditions.

#### Normal tissue toxicity to inverse fluence rate × photosensitizer dosing

Lastly, a toxicity assay was used to evaluate the normal tissue response to isoeffective regimens of inverse fluence rate ×

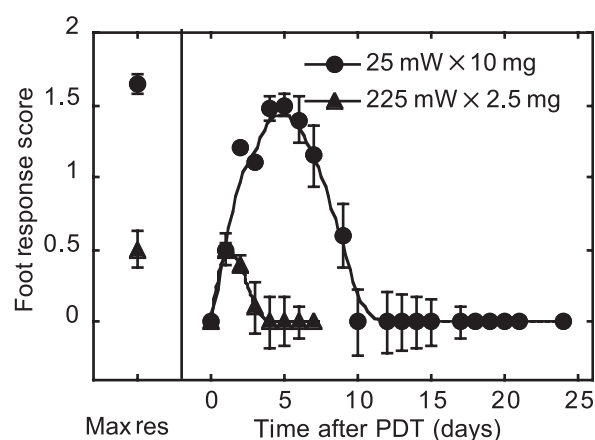


**Figure 5.** Normal tissue toxicity to PDT at 25 mW cm<sup>-2</sup>, 10 mg kg<sup>-1</sup> Photofrin (25 mW × 10 mg) and 225 mW cm<sup>-2</sup>, 2.5 mg kg<sup>-1</sup> Photofrin (225 mW × 2.5 mg). Illumination (630 nm) was for 30 min at ~24 h after i.v. Photofrin injection. Foot-response scores are described in Table 1 of the Materials and Methods. Maximum response (Max res) indicates the median (±SE) of the highest score observed in each animal regardless of the day on which this response occurred. Line plots depict median (±SE) score as a function of day after PDT; the 0 day reading was a baseline observation before PDT. *n* = 10 animals/condition.

photosensitizer dose pairing. Figure 5 displays murine foot response to PDT at 25 mW × 10 mg and 225 mW × 2.5 mg. PDT at 25 mW × 10 mg clearly produced a strong normal tissue response, demonstrated by a maximum score (med-

ian  $\pm$  SE) of  $1.65 \pm 0.07$ . A median ( $\pm$ SE) of  $10 \pm 2$  days was needed for complete resolution of tissue damage after PDT at  $25 \text{ mW} \times 10 \text{ mg}$ . In contrast,  $225 \text{ mW} \times 2.5 \text{ mg}$  resulted in a maximum score (median  $\pm$  SE) of  $0.5 \pm 0.13$  and a median ( $\pm$ SE) of  $4 \pm 0.6$  days to resolution. The difference in foot response to these regimens was significant ( $P < 0.0006$ ) in terms of both the peak and duration of response. No response was observed in control feet exposed to only photosensitizer ( $10 \text{ mg kg}^{-1}$  Photofrin), only light ( $225 \text{ mW cm}^{-2}$ ) or untreated.

Although normal tissue toxicity between the extreme isoeffective regimens was strikingly different, an intermediate isoeffective regimen ( $75 \text{ mW} \times 5 \text{ mg}$ ) did not result in intermediate toxicity. Rather, at  $75 \text{ mW} \times 5 \text{ mg}$  normal tissue toxicity was reduced dramatically compared with toxicity at  $25 \text{ mW} \times 10 \text{ mg}$ . The median response at  $75 \text{ mW} \times 5 \text{ mg}$  (maximum score 0.45; 4 days to resolution) was indistinguishable from response to  $225 \text{ mW} \times 2.5 \text{ mg}$ .

## DISCUSSION

The data of this report demonstrate that high fluence rate PDT can be carried out under oxygen-conserving conditions by combining the high rate with low photosensitizer dose. Although complete preservation of pre-PDT oxygen levels was not achieved at the highest fluence rate tested, significant direct cell kill occurred in the absence of substantial normal tissue toxicity and tumor response was as durable as that found for the more oxygen-conserving regimens. The relevance of tumor oxygen levels to the high fluence rate  $\times$  low photosensitizer dose regimens was confirmed by the presence of highly significant associations between PDT effect on tumor hemoglobin oxygen saturation (*relative-SO<sub>2</sub>*) and response durability (time-to-400 mm<sup>3</sup>).

High fluence rate PDT offers the clinical advantage of shorter illumination times, thus these data are of direct clinical relevance. The drug doses needed for oxygen-conserving yet efficacious high fluence rate PDT (*e.g.*  $2.5\text{--}3.5 \text{ mg kg}^{-1}$ ) are no lower than those already commonly applied in the clinic. These findings emphasize the need for measurement of tissue oxygenation and photosensitizer levels during clinical applications of PDT. In studies performed to date, highly variable levels of PDT-created hypoxia have been detected both within and among patients receiving identical PDT regimens (18,31,32). Intertissue variability in photosensitizer levels has been suggested as an explanation for these findings (31), but no attempts to correlate photosensitizer levels and PDT oxygen depletion in the same tumor sample have been made. We intend to study these variables in our upcoming clinical trials.

These data also demonstrate that time-conserving PDT can be carried out at low fluence rate by increasing the photosensitizer dose. In other words, higher photosensitizer dose facilitated the use of low fluence rate without a need to increase treatment time. Although some models have suggested that it may be possible to utilize oxygen-conserving low fluence rates without extension of treatment time (33), in preclinical applications longer treatment times are required at low fluence rate to compensate for the slower rate of light delivery compared with high fluence rate (6). Unfortunately, our data show that tumor response gained by increasing photosensitizer dose at low fluence rate came at a cost of

greater damage to normal tissue. Therefore, this approach to controlling treatment time at low fluence rate is not clinically favorable.

Although therapeutic efficacy was similar at the high and low fluence rates we studied, these regimens evoked different mechanisms of action. During PDT at  $25 \text{ mW} \times 10 \text{ mg}$  direct cell kill was limited, as indicated by small decreases in tumor cell clonogenicity immediately after PDT. Ultimately, indirect mechanisms of cell kill, potentially including vascular, immune or other host effects were sufficient to create a durable tumor response. Indeed, a reduction in THC at the conclusion of PDT suggests that tumor perfusion decreased during PDT and the presence of a significant decrease in tumor clonogenicity by 17 h after PDT suggests that indirect PDT effects ultimately impact treatment response. However, substantial normal tissue toxicity was also created by  $25 \text{ mW} \times 10 \text{ mg}$  PDT, most likely as a result of a prominent vascular component to this treatment. Reducing the photosensitizer dose to  $5 \text{ mg kg}^{-1}$  at  $25 \text{ mW cm}^{-2}$  enabled better maintenance of THC at treatment conclusion (data not shown), but it also rendered the treatment ineffective, with a response durability similar to control response. Together these data suggest that vascular effects, which are likely a consequence of the high photosensitizer dose, are an essential component of the response to low fluence rate  $\times$  high photosensitizer regimens.

Vascular effects during  $25 \text{ mW} \times 10 \text{ mg}$  PDT are expected to have limited direct cell kill. However, tumor hemoglobin oxygen saturation was not depleted during PDT (*relative-SO<sub>2</sub>*  $> 1$ ). Thus, although total tumor blood flow decreased during illumination, those vessels with flow remained well oxygenated. It is possible for vascular perfusion to decrease in the absence of an effect on *SO<sub>2</sub>* because *SO<sub>2</sub>* reflects the oxygenation status of vessels with blood flow without direct consideration of any change in the number of vessels with flow.

During PDT at  $225 \text{ mW} \times 2.5 \text{ mg}$ , a significant amount of direct tumor cell kill occurred. This was likely aided by preservation of blood flow during treatment as no PDT effect on THC was detected with this treatment protocol. A minor but statistically significant decrease in *relative-SO<sub>2</sub>* occurred during  $225 \text{ mW} \times 2.5 \text{ mg}$  PDT. The depletion of tumor hemoglobin oxygen saturation suggests that some photochemical consumption of oxygen occurred during treatment. Nevertheless, *SO<sub>2</sub>* was maintained at  $\sim 85\%$  of its baseline value, and the extent of consumption did not significantly alter response durability compared with other effective treatment protocols, nor did it prevent the occurrence of significant direct cell kill. When photosensitizer dose was lowered to  $1.0 \text{ mg kg}^{-1}$  tumor response was significantly abrogated, suggesting limitations in tumor drug levels.

This investigation is unique from other investigations of fluence rate effects because we used constant treatment time and varied photosensitizer and light dose, whereas others have typically used a constant photosensitizer and light dose and varied treatment time. Due to these differences in study design, we have found a different spectrum of fluence rate-dependent tissue responses than those previously reported. Our use of a high drug dose led to acute vascular effects and limited direct cell kill for our low fluence rate regimen. In published studies, low fluence rate is associated with

substantial direct cell kill and delayed vascular effects (2,34–36). This suggests that increasing the photosensitizer dose may have altered the time frame of vascular damage development. When we used a low drug dose in combination with high fluence rate, minimal oxygen depletion, significant direct cell kill and a durable tumor response were found. In published studies, high fluence rate is associated with limited cell kill and abrogated tumor response (2,4,13). Therefore, decreasing the photosensitizer dose at high fluence rate may increase the contribution of direct cytotoxicity to tumor response.

PDT effect on tumor oxygenation was studied as a function of changes in tumor hemoglobin oxygen saturation ( $SO_2$ ). Higher  $SO_2$  at the conclusion of PDT predicted for a more durable tumor response; in fact all animals with *relative-SO<sub>2</sub>* values  $\geq 2$  ( $n = 5$ ) required at least 21 days for tumor regrowth to 400 mm<sup>3</sup> ( $n = 2$ ) or were cured ( $n = 3$ ). This includes the one animal that was cured after PDT at 225 mW  $\times$  1 mg ( $SO_2$  data not shown). On average, only the 75 mW  $\times$  5 mg condition led to a significant increase in *relative-SO<sub>2</sub>*, which was likely a result of decreases in metabolic oxygen consumption as some direct cytotoxicity (data not shown) was found with this treatment. However, 225 mW  $\times$  2.5 mg was associated with both significant direct cytotoxicity and a modest decrease in *relative-SO<sub>2</sub>*. In this case, the decrease in  $SO_2$  could be attributed to photochemical oxygen consumption, which was likely attenuated by an increase in  $SO_2$  due to reduced metabolic oxygen consumption. Therefore, change in  $SO_2$  during PDT appears to represent a balance between increases due to cell death (reduced metabolic oxygen consumption) and decreases due to photochemical oxygen consumption.

Vascular effects can also be expected to play some part in determining  $SO_2$ , but it is important to reiterate that  $SO_2$  reflects the oxygenation status of hemoglobin, so constricted vessels void of hemoglobin will not contribute to the measured signal. In other words, regional hypoxia created by the local shutdown of vessels during PDT will not be reflected by  $SO_2$  measurement unless vascular shutdown is extensive enough to lead to greater tumor-averaged extraction of  $O_2$  from the hemoglobin of perfused blood vessels. Therefore, PDT-induced changes in blood flow can occur independent of a corresponding effect on  $SO_2$  (32), which explains why 25 mW  $\times$  10 mg PDT demonstrated decreases in vascular perfusion and limitations in direct cell kill, but no effect on  $SO_2$ .

The change in tumor  $SO_2$  during identical PDT conditions was variable, despite the fact that tumors from the same cell solution were implanted on inbred animals. This finding can perhaps be explained by intertumor heterogeneity in Photofrin uptake. Drug uptake could vary substantially among tumors, especially those exposed to the higher photosensitizer doses. The standard error in drug uptake was 3.7 ng mg<sup>-1</sup> among mice receiving an injected dose of 10 mg kg<sup>-1</sup> (average drug uptake 13 ng mg<sup>-1</sup>), whereas the standard error was 0.08 ng mg<sup>-1</sup> among mice receiving an injected dose of 2.5 mg kg<sup>-1</sup> (average drug uptake 1.3 ng mg<sup>-1</sup>). At the lower drug doses especially, photobleaching during PDT could further reduce intertumor variability in drug levels or even lead to complete drug depletion. Less variability in  $SO_2$  response during PDT was

found for regimens using lower photosensitizer doses (compare panels a and d of Fig. 3), which suggests that  $SO_2$  response and intra- and/or intertumor variability in photosensitizer levels are related. A dedicated investigation of Photofrin uptake and photobleaching will be needed to confirm these expectations.

The highly significant correlations between *relative-SO<sub>2</sub>* and response durability (time-to-400 mm<sup>3</sup>) as found in these studies are a valuable addition to previous publications by ourselves (17) and others (37), which identify PDT effect on tumor oxygenation as an individualized predictor of treatment outcome. In the present manuscript, we demonstrate that the PDT-induced change in hemoglobin oxygen saturation is predictive of tumor response over a range of Photofrin-PDT conditions, including those that create damage through different mechanisms of action. Data from all response-producing protocols were well fit by a single model relating *relative-SO<sub>2</sub>* and response durability. This suggests that the utility of  $SO_2$  monitoring is not protocol specific among regimens of Photofrin-PDT. Not surprisingly, however, the data also show that  $SO_2$  monitoring is of little value for ineffectual PDT protocols: if the photosensitizer and illumination conditions are insufficient to elicit a PDT response then optimization of the physiological environment is to no avail, albeit one would also expect to no harm. Therefore, these results support continued development of  $SO_2$  monitoring during Photofrin-PDT as a method of real time dosimetry with the potential to individualize patient treatment toward the goals of reduced morbidity and increased efficacy. Such techniques are currently being pursued in the clinical setting by several groups, including ourselves (32,38–41).

In summary, this report presents the results of a unique investigation that identifies how manipulation of photosensitizer dose in combination with fluence rate can be used to control oxygen depletion and enhance therapeutic efficacy. Among the inverse fluence rate  $\times$  photosensitizer dose pairs studied, we have found high fluence rate in combination with low photosensitizer dose to provide efficacious tumor response in the absence of significant normal tissue toxicity. Such a regimen is readily adaptable to the clinic where low drug dose and high fluence rate are generally considered desirable for the sake of reduced skin photosensitivity and more rapid treatment, respectively. The importance of oxygen maintenance to the success of inverse fluence rate  $\times$  photosensitizer dose pairs, including high fluence rate  $\times$  low photosensitizer dose, was confirmed by its highly significant correlation to tumor response. Therefore, the translation of these results to clinical applications is readily feasible through use of oxygen and photosensitizer monitoring technologies, which are under intense development.

*Acknowledgements*—This work was supported by NIH grants RO1 CA-85831 and PO1 CA-87971. We thankfully acknowledge Carmen Rodriquez for technical assistance with laser maintenance.

## REFERENCES

- Henderson, B. W., T. M. Busch and J. W. Snyder (2006) Fluence rate as a modulator of PDT mechanisms. *Lasers Surg. Med.* **38**, 489–493.

2. Sitnik, T. M., J. A. Hampton and B. W. Henderson (1998) Reduction of tumour oxygenation during and after photodynamic therapy *in vivo*: Effects of fluence rate. *Br. J. Cancer*. **77**, 1386–1394.
3. Henderson, B. W., S. O. Gollnick, J. W. Snyder, T. M. Busch, P. C. Kousis, R. T. Cheney and J. Morgan (2004) Choice of oxygen-conserving treatment regimen determines the inflammatory response and outcome of photodynamic therapy of tumors. *Cancer Res.* **64**, 2120–2126.
4. Coutier, S., L. N. Bezdetnaya, T. H. Foster, R. M. Parache and F. Guillemin (2002) Effect of irradiation fluence rate on the efficacy of photodynamic therapy and tumor oxygenation in meta-tetra (hydroxyphenyl) chlorin (mTHPC)-sensitized HT29 xenografts in nude mice. *Radiat. Res.* **158**, 339–345.
5. Angell-Petersen, E., S. Spetalen, S. J. Madsen, C. H. Sun, Q. Peng, S. W. Carper, M. Sioud and H. Hirschberg (2006) Influence of light fluence rate on the effects of photodynamic therapy in an orthotopic rat glioma model. *J. Neurosurg.* **104**, 109–117.
6. Sitnik, T. M. and B. W. Henderson (1998) The effect of fluence rate on tumor and normal tissue responses to photodynamic therapy. *Photochem. Photobiol.* **67**, 462–466.
7. Ericson, M. B., C. Sandberg, B. Stenquist, F. Gudmundson, M. Karlsson, A. M. Ros, A. Rosen, O. Larko, A. M. Wennberg and I. Rosdahl (2004) Photodynamic therapy of actinic keratosis at varying fluence rates: Assessment of photobleaching, pain and primary clinical outcome. *Br. J. Dermatol.* **151**, 1204–1212.
8. Foster, T. H., R. S. Murrant, R. G. Bryant, R. S. Knox, S. L. Gibson and R. Hilf (1991) Oxygen consumption and diffusion effects in photodynamic therapy. *Radiat. Res.* **126**, 296–303.
9. Henning, J. P., R. L. Fournier and J. A. Hampton (1995) A transient mathematical model of oxygen depletion during photodynamic therapy. *Radiat. Res.* **142**, 221–226.
10. Pogue, B. W. and T. Hasan (1997) A theoretical study of light fractionation and dose-rate effects in photodynamic therapy. *Radiat. Res.* **147**, 551–559.
11. Foster, T. H. and L. Gao (1992) Dosimetry in photodynamic therapy: Oxygen and the critical importance of capillary density. *Radiat. Res.* **130**, 379–383.
12. Busch, T. M., E. P. Wileyto, M. J. Emanuele, F. Del Piero, L. Marconato, E. Glatstein and C. J. Koch (2002) Photodynamic therapy creates fluence rate-dependent gradients in the intratumoral spatial distribution of oxygen. *Cancer Res.* **62**, 7273–7279.
13. Inuma, S., K. T. Schomacker, G. Wagnieres, M. Rajadhyaksha, M. Bamberg, T. Momma and T. Hasan (1999) *In vivo* fluence rate and fractionation effects on tumor response and photobleaching: Photodynamic therapy with two photosensitizers in an orthotopic rat tumor model. *Cancer Res.* **59**, 6164–6170.
14. Georgakoudi, I., M. G. Nichols and T. H. Foster (1997) The mechanism of Photofrin photobleaching and its consequences for photodynamic dosimetry. *Photochem. Photobiol.* **65**, 135–144.
15. Yuan, J., P. A. Mahama-Relue, R. L. Fournier and J. A. Hampton (1997) Predictions of mathematical models of tissue oxygenation and generation of singlet oxygen during photodynamic therapy. *Radiat. Res.* **148**, 386–394.
16. Busch, T. M., S. M. Hahn, E. P. Wileyto, C. J. Koch, D. L. Fraker, P. Zhang, M. Putt, K. Gleason, D. B. Shin, M. J. Emanuele, K. Jenkins, E. Glatstein and S. M. Evans (2004) Hypoxia and Photofrin uptake in the intraperitoneal carcinoma-tosis and sarcomatosis of photodynamic therapy patients. *Clin. Cancer Res.* **10**, 4630–4638.
17. Wang, H. W., M. E. Putt, M. J. Emanuele, D. B. Shin, E. Glatstein, A. G. Yodh and T. M. Busch (2004) Treatment-induced changes in tumor oxygenation predict photodynamic therapy outcome. *Cancer Res.* **64**, 7553–7561.
18. Wang, H. W., T. C. Zhu, M. E. Putt, M. Solonenko, J. Metz, A. Dimofte, J. Miles, D. L. Fraker, E. Glatstein, S. M. Hahn and A. G. Yodh (2005) Broadband reflectance measurements of light penetration, blood oxygenation, hemoglobin concentration, and drug concentration in human intraperitoneal tissues before and after photodynamic therapy. *J. Biomed. Opt.* **10**, 14004.
19. Solonenko, M., R. Cheung, T. M. Busch, A. Kachur, G. M. Griffin, T. Vulcan, T. C. Zhu, H. W. Wang, S. M. Hahn and A. G. Yodh (2002) *In vivo* reflectance measurement of optical properties, blood oxygenation and motexafin lutetium uptake in canine large bowels, kidneys and prostates. *Phys. Med. Biol.* **47**, 857–873.
20. Menon, C., G. M. Polin, I. Prabhakaran, A. Hsi, C. Cheung, J. P. Culver, J. F. Pingpank, C. S. Sehgal, A. G. Yodh, D. G. Buerk and D. L. Fraker (2003) An integrated approach to measuring tumor oxygen status using human melanoma xenografts as a model. *Cancer Res.* **63**, 7232–7240.
21. Wang, H.-W., T. Zhu, M. Solonenko, S. M. Hahn, J. M. Metz, A. Dimofte, J. Miles and A. G. Yodh (2003) *In-vivo* measurements of penetration depth, oxygenation, and drug concentration using broadband absorption spectroscopy in human tissues before and after photodynamic therapy. *Proc. SPIE* **4952**, 68–75.
22. Prahl, S. (2005) *Optical properties spectra*. Available at: <http://omlc.ogi.edu/spectra/index.html>. Accessed on 15 December 2005.
23. Haskell, R. C., L. O. Svaasand, T. T. Tsay, T. C. Feng, M. S. McAdams and B. J. Tromberg (1994) Boundary conditions for the diffusion equation in radiative transfer. *J. Opt. Soc. Am. A Opt. Image Sci. Vis.* **11**, 2727–2741.
24. Kienle, A. and M. S. Patterson (1997) Improved solutions of the steady-state and the time-resolved diffusion equations for reflectance from a semi-infinite turbid medium. *J. Opt. Soc. Am. A Opt. Image Sci. Vis.* **14**, 246–254.
25. Hull, E. L., M. G. Nichols and T. H. Foster (1998a) Quantitative broadband near-infrared spectroscopy of tissue-simulating phantoms containing erythrocytes. *Phys. Med. Biol.* **43**, 3381–3404.
26. Hull, E. L., M. G. Nichols and T. H. Foster (1998b) Localization of luminescent inhomogeneities in turbid media with spatially resolved measurements of CW diffuse luminescence emittance. *Appl. Opt.* **37**, 2755–2765.
27. Choe, R., T. Durduran, G. Yu, M. J. Nijland, B. Chance, A. G. Yodh and N. Ramanujam (2003) Transabdominal near infrared oximetry of hypoxic stress in fetal sheep brain in utero. *Proc. Natl Acad. Sci. USA* **100**, 12950–12954.
28. Culver, J. P., T. Durduran, D. Furuya, C. Cheung, J. H. Greenberg and A. G. Yodh (2003) Diffuse optical tomography of cerebral blood flow, oxygenation, and metabolism in rat during focal ischemia. *J. Cereb. Blood Flow* **23**, 911–924.
29. Durduran, T., R. Choe, J. P. Culver, L. Zubkov, M. J. Holboke, J. Giannarino, B. Chance and A. G. Yodh (2002) Bulk optical properties of healthy female breast tissue. *Phys. Med. Biol.* **47**, 2847–2861.
30. Corlu, A., T. Durduran, R. Choe, M. Schweiger, E. M. Hillman, S. R. Arridge and A. G. Yodh (2003) Uniqueness and wavelength optimization in continuous-wave multispectral diffuse optical tomography. *Opt. Lett.* **28**, 2339–2341.
31. Henderson, B. W., T. M. Busch, L. A. Vaughan, N. P. Frawley, D. Babich, T. A. Sosa, J. D. Zollo, A. S. Dee, M. T. Cooper, D. A. Bellnier, W. R. Greco and A. R. Oseroff (2000) Photofrin photodynamic therapy can significantly deplete or preserve oxygenation in human basal cell carcinomas during treatment, depending on fluence rate. *Cancer Res.* **60**, 525–529.
32. Yu, G., T. Durduran, C. Zhou, T. Zhu, J. C. Finlay, T. M. Busch, S. B. Malkowicz, S. M. Hahn and A. G. Yodh (2006) Real-time in situ monitoring of human prostate photodynamic therapy with diffuse light. *Photochem. Photobiol.* **82**, 1279–1284.
33. Langmack, K., R. Mehta, P. Twyman and P. Norris (2001) Topical photodynamic therapy at low fluence rates—theory and practice. *J. Photochem. Photobiol. B* **60**, 37–43.
34. Sitnik, T. M. and B. W. Henderson (1997) Effects of fluence rate on cytotoxicity during photodynamic therapy. *Proc. SPIE* **2972**, 95–102.
35. Madsen, S. J., C. H. Sun, B. J. Tromberg, V. P. Wallace and H. Hirschberg (2000) Photodynamic therapy of human glioma spheroids using 5-aminolevulinic acid. *Photochem. Photobiol.* **72**, 128–134.
36. Seshadri, M., J. A. Sperryak, R. Mazurchuk, S. H. Camacho, A. R. Oseroff, R. T. Cheney and D. A. Bellnier (2005) Tumor vascular response to photodynamic therapy and the antivascular agent 5,6-dimethylxanthone-4-acetic acid: Implications for combination therapy. *Clin. Cancer Res.* **11**, 4241–4250.
37. Pham, T. H., R. Hornung, M. W. Berns, Y. Tadir and B. J. Tromberg (2001) Monitoring tumor response during photodynamic therapy using near-infrared photon-migration spectroscopy. *Photochem. Photobiol.* **73**, 669–677.

38. Zhu, T. C., J. C. Finlay and S. M. Hahn (2005) Determination of the distribution of light, optical properties, drug concentration, and tissue oxygenation in-vivo in human prostate during motexafin lutetium-mediated photodynamic therapy. *J. Photochem. Photobiol. B* **79**, 231–241.
39. Cottrell, W. J., A. R. Oseroff and T. H. Foster (2006a) Portable instrument that integrates irradiation with fluorescence and reflectance spectroscopies during clinical photodynamic therapy of cutaneous disease. *Rev. Sci. Instrum.* **77**, 064302.
40. Cottrell, W. J., A. R. Oseroff and T. H. Foster (2006b) System for providing simultaneous PDT delivery and dual spectroscopic monitoring in clinical basal cell carcinoma therapy. *Proc. SPIE* **6139**, 613918-1–613918-10.
41. Weersink, R. A., A. Bogaards, M. Gertner, S. R. Davidson, K. Zhang, G. Netchev, J. Trachtenberg and B. C. Wilson (2005) Techniques for delivery and monitoring of TOOKAD (WST09)-mediated photodynamic therapy of the prostate: Clinical experience and practicalities. *J. Photochem. Photobiol. B* **79**, 211–222.